Article

High-Throughput Monitoring of Bacterial Cell Density in Nanoliter Droplets: Label-Free Detection of Unmodified Gram-Positive and Gram-Negative Bacteria

Natalia Pacocha, Jakub Bogusławski, Michał Horka, Karol Makuch, Kamil Liżewski, Maciej Wojtkowski, and Piotr Garstecki*
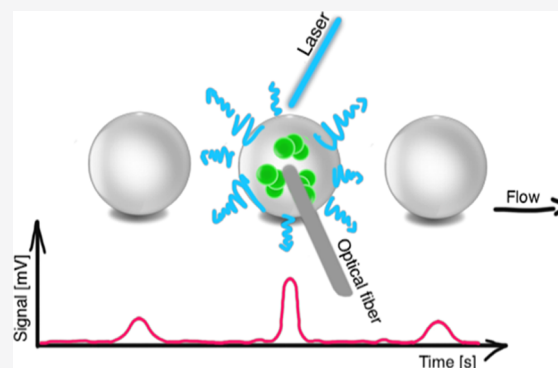
Read Online

ACCESS | Metrics & More | Article Recommendations | Supporting Information

ABSTRACT: Droplet microfluidics disrupted analytical biology with the introduction of digital polymerase chain reaction and single-cell sequencing. The same technology may also bring important innovation in the analysis of bacteria, including antibiotic susceptibility testing at the single-cell level. Still, despite promising demonstrations, the lack of a high-throughput label-free method of detecting bacteria in nanoliter droplets prohibits analysis of the most interesting strains and widespread use of droplet technologies in analytical microbiology. We use a sensitive and fast measurement of scattered light from nanoliter droplets to demonstrate reliable detection of the proliferation of encapsulated bacteria. We verify the sensitivity of the method by simultaneous readout of fluorescent signals from bacteria expressing fluorescent proteins and demonstrate label-free readout on unlabeled Gram-negative and Gram-positive species. Our approach requires neither genetic modification of the cells nor the addition of chemical markers of metabolism. It is compatible with a wide range of bacterial species of clinical, research, and industrial interest, opening the microfluidic droplet technologies for adaptation in these fields.

Droplet microfluidics has already proven to be useful in many analytical methods in chemistry and biology, including digital polymerase chain reaction[1] and single-cell sequencing.[2] The technology allows to culture bacteria in droplets,[3] count colony forming units (cfus) in a digital assay format,[4] and probe antibiotic susceptibility at a single-cell level.[5–] Another example is screening the inoculum effect, that is, the impact of bacterial cell density variation on their collective level of antibiotic resistance.[6–78] These demonstrations have been enabled by unique advantages of droplet-based methods, including miniaturization, low cost, a small volume of operations, lower reagent consumption, and potential for high-throughput operation. Having said capabilities, droplet technology can offer a faster, more accessible, and cost-effective alternative to classical antibiotic susceptibility testing.[9] The ability to work with millions of replicates of the sample, crucial in microbiological experiments, ensures the reliability of determining the results, but on the other hand, it creates a high demand for a high-throughput analytical method for detection.

Despite the significant progress in droplet generation methods, where frequency for parallelized microfluidic droplet generators of pico- and nanoliter compartments reaches hundreds of kHz,[10–13] the detection methods have lagged. The most general approach is based on detecting fluorescence light; however, bacteri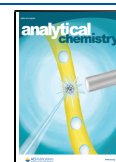a do not naturally produce strong fluorescence signals. Some additional steps have to be taken to modify cells or their environment, which in each case has some disadvantages. For example, an addition of fluorescence dye can result in dye leakage, making bacteria growth detection either impossible or limiting available incubation time.[14–16] Genetic modification, on the other hand, is very complicated and not applicable in every laboratory. On the contrary, label-free detection methods allow one to work with any bacterial species without additional steps. Thus, there is an essential need for the development of label-free techniques that would allow for detecting the proliferation of unlabeled bacteria in droplets.

Some steps toward this goal have already been taken. For example, Boitard et al. presented an interesting method for cell detection in picodroplets.[17] The droplet composition changes during bacterial growth, which results in a change of osmotic pressure. Water molecules start to migrate between droplets
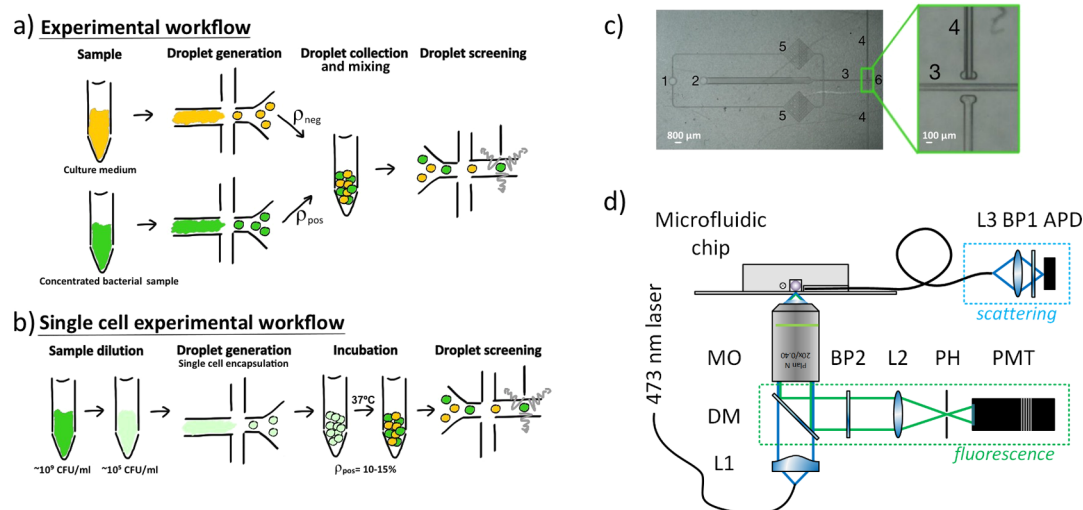
Figure 1. Overview of experimental workflows and setup, (a) scheme of the experimental workflow, (b) scheme of the experimental workflow for single-cell experiments, (c) micrograph showing the microfluidic chip with the flow-focusing junction for droplet screening; 1-inlet for continuous phase, 2-inlet for droplets, 3-detection channel, 4-guiding channels for optical fiber, 5-filters, and 6-outlet, (d) schematic of the optical setup; L1-lens no. 1, L2-lens no. 2, L3-lens no. 3, DM-dichroic mirror, PH-pinhole, PMT-photomultiplier, MO-microscope objective, BP1-bandpass filter no. 1, BP2-bandpass filter no. 2, and APD-avalanche photodiode.

causing their shrinking or swelling. The decrease in volume correlates with the number of cells. Unfortunately, the method did not provide a high-throughput screening of the droplets. Similarly, Liao et al. showed a label-free and sensitive method for bacterial detection in picoliter droplets using micro-Raman spectroscopy, but the technique was not used for droplet screening.[18] In another example, Jakiela et al.[19] presented a method for measuring the optical density of larger droplets (ca. microliter volume) through measuring the light absorption. While these results show that, in principle, the readout of optical density in droplets is possible, the droplets' size makes high-throughput applications challenging. On the other hand, Zang et al.[20] presented a method for detecting bacteria's growth in picoliter droplets based on real-time image processing. They achieved a 100 Hz frequency of readout and growth-dependent droplet sorting.

An alternative to the methods mentioned above is the detection of scattering. It poses a great advantage of being inherently label-free and should work with any bacterial species with high-throughput. In this scheme, bacterial cells inside the droplets are illuminated with a laser beam, which changes its direction of propagation upon scattering. The intensity of scattered light is directly proportional to the number of scatterers—in this case, bacterial cells. This technique has been used by Liu et al.[21] to detect the light scattered by bacterial cells in picoliter droplets. The setup utilizes fiber optic components for light collection, which makes it more compact and cost-effective. The screening frequency was 243 Hz, and it took 13 h to analyze a library composed of 11 million picodroplets. Similarly, Hengoju et al. presented an optofluidic detection system based on the readout of absorbance and scattered light in picoliter droplets.[22] The droplet screening was conducted with a frequency of approx. 40 Hz. Both the approaches mentioned above do provide tests for *Escherichia coli* and *Streptomyces hygroscopicus* cells only. The task to provide sufficient tests for this technique for different microbiological samples still needs to be accomplished.

Here, we demonstrate a high-throughput and label-free method for monitoring the bacteria growth in nanoliter

droplets. In our approach, we measure the intensity of scattered light, which provides high versatility of analyzed samples. The method extends the throughput screening up to frequencies over 1.2 kHz. We confirmed that the method is compatible with different species of bacteria (*Escherichia coli, Pseudomonas aeruginosa, Corynebacterium simulans, Staphylococcus aureus, Staphylococcus intermedius, Klebsiella pneumoniae, Acinetobacter baumanii, Salmonella arizonae, Shigella sonnei,* and *Listeria monocytogenes*), which represents various structures, shapes, and growth characteristics. Moreover, our setup allows for simultaneous reading of fluorescence. The results obtained in the scattering channel are in excellent correlation to data received from fluorescence analysis. After successfully verifying the system's performance, we demonstrated its application in microbiological experiments, that is, to study minimum inhibitory concentration at the single-cell level (scMIC) and phenotypic heterogeneity of bacteria population. The microbial studies are performed on *S. aureus*, which is of great clinical interest. Our experiments confirmed that scattering-based detection could be used for fast and reliable analysis of various bacterial species and study each cell's behavior in the bacterial population after antibiotic treatment.

■ EXPERIMENTAL SECTION

Microfluidic Chip Fabrication. Microfluidic chips for the generation of droplets and the reading of fluorescence and scattered light intensities (see Supporting Information for more details about chips designs) were made in three steps. First, the channels were milled in a polycarbonate (PC) plate using a CNC machine (MSG4025, Ergwind, Poland). In the second step, polydimethylsiloxane (PDMS) mold was produced by pouring PDMS onto the PC chip, polymerization at 75 °C for 1 h, activating the surface by Laboratory Corona Treater (BD 20AC, Electro-Technic Products, USA) and silanizing in the vapors of tridecafluoro-1,1,2,2-tetrahydrooctyl-1-trichlorosilane (United Chemical Technologies, USA) for 30 min under 10 mbar pressure. In the last step, the prepared silanized mold was used to fabricate PDMS chips, which were finally bonded to 1 mm thick glass slides using oxygen plasma.

The hydrophobicity of the microfluidic channels was provided by introducing modifying solution Novec 1720 (3M, USA), evaporation at room temperature, and baking the chips at 75 °C for 1 h.

Experimental Workflow. A schematic description of the experimental workflow used in this work is presented in Figure 1a. A validation of our system was performed by analyzing samples containing different ratios of droplets containing culture medium only (negative) and the droplets containing a high concentration of bacteria (positive). Negative droplets were formed by the encapsulation of culture medium, and positive compartments were formed using an overnight bacterial sample. Samples were split into 1 nL droplets using a flow-focusing chip (see Figure S1) and neMESYS syringe pumps (Cetoni, Germany) with a frequency of ∼500 Hz. Afterward, both negative and positive droplets in known proportions were collected in a 1.5 mL Eppendorf tube and mixed by gentle rotations. The percentage content of positive droplets in the sample is indicated by ρ_{pos}, while the percentage content of negatives is indicated by ρ_{neg}.

Single-Cell Experimental Workflow. Figure 1b presents a workflow for experiments performed at the single-cell level. The bacterial sample was first diluted to a concentration of 10^5 cfu/mL. It provides a high probability of single-cell encapsulation. Droplets were generated with the microfluidic chip mentioned above and collected in a 1.5 mL Eppendorf tube for incubation at 37 °C in the microbiological incubator (Thermo Scientific, USA).

Optical Setup and Droplet Screening. The general principle of operation is based on Mie scattering theory, where bacterial cells can be approximated by spheroids with a size roughly comparable to the wavelength of light. The scattered light changes the direction of propagation and can be collected with an optical fiber positioned off the optical axis, in this case, perpendicularly to the laser beam. The intensity of scattered light is proportional to the number of scatterers, that is, bacterial cells, and allows us for quantification of bacterial density. We also included the fluorescence detection channel to confirm whether the detection of scattered light provides the same information as well-established detection of fluorescence.

Our droplet screening system is based on a microfluidic chip with a flow-focusing junction, shown in Figure 1c. The droplets enter the microfluidic chip through an inlet channel on the left side. Next, two additional oil streams without a surfactant dilute the droplets to separate them further apart from each other in the detection channel. The additional oil also dilutes the high concentration of surfactant in the original emulsion. This way, we decrease the background scattering signal on the continuous liquid. Finally, the droplets get to the main detection channel, where they are illuminated by the focused laser beam.

Figure 1d shows the complete optical setup. A 473 nm laser beam delivered by a fiber is first collimated with a lens (L1, focal length 19 mm) and then focused by a 20× objective (MO, Olympus RMS20X) into the middle of the detection channel. The scattered light is collected with a multimode optical fiber positioned at an angle of 90° with respect to the laser beam. We use a 105 μm fiber with a low numerical aperture (0.1) to restrain the detection area. An aspheric lens then focuses the guided light (L2, focal length 8 mm) onto an avalanche photodiode (APD, Thorlabs APD120A, bandwidth: 50 MHz). We use a bandpass filter (central wavelength of 470 and 10 nm of bandwidth) to filter out the fluorescence and

pass the scattered light only. The fluorescence signal collected by the objective is reflected on a dichroic mirror (DM, a cut-off wavelength of 490 nm), passes a bandpass filter (BP, a central wavelength of 530 and 43 nm of bandwidth), and then the light is focused by a lens (L3, focal length 30 mm), passes a pinhole, and targets a photomultiplier (PMT, Hamamatsu H5783-20). The PMT is placed in confocal configuration, which allows rejecting out-of-focus light (e.g., light reflected from other surfaces, stray light). Both collected signals are recorded simultaneously with the data acquisition card (National Instruments, USB-6212, sampling frequency: 500 kHz) and processed by custom-written LabVIEW software. Simultaneous detection of both channels allows us to analyze correlations between signals at a single-droplet level.

Screening of Bacteria toward Heterogeneity. Phenotypic heterogeneity of *S. aureus* was tested based on the determination of single-cell minimum inhibitory concentrations of gentamicin. Bacteria from an overnight culture were diluted and incubated at 37 °C to OD_{600} 0.2. Then, bacterial suspension was diluted to the concentration of 10^5 cfu/mL, and a series of antibiotic dilutions were added. Each sample was split into 1 nL droplets, collected in 1.5 mL Eppendorf tubes, and incubated at 37 °C in the microbiological incubator for 18 h. After incubation, droplets were screened with our label-free system in five replicates for each antibiotic concentration. The percentage of positive droplets was determined, which was a base for further analysis towards heterogeneity of the tested bacteria population. A detailed description of the numerical analysis of data toward heterogeneity is included in Supporting Information.

Reagents. Chip fabrication: PDMS precursor and initiator (Dow Corning, USA) and tridecafluoro-1,1,2,2-tetrahydrooctyl-1-trichlorosilane (United Chemical Technologies, USA), Novec 1720 (3M, USA). Generation and reading of droplets: Novec HFE 7500 fluorocarbon oil (3M, USA) and triblock PFPE−PEG−PFPE surfactant. Antibiotic kill tests: gentamicin (Sigma-Aldrich, USA).

Bacteria. We used twelve species of bacteria: *E. coli* ATCC 25922, *E. coli* TOP 10 placEGFP, *S. aureus* NCTC 8325-4, *S. aureus* SH1000, *C. simulans* DSM 44392, *P. aeruginosa* ATCC 27353, *S. intermedius* ATCC 29663, *K. pneumoniae* ATCC 13883, *Acinetobacter baumannii* ATCC 19606, *Salmonella arizonae* ATCC 13314, *S. sonnei* ATCC 29930, and *L. monocytogenes* ATCC 1915. Bacteria were cultured in Tryptic Soy Broth (Biocorp, Poland) or Brain Heart Infusion media (Biocorp, Poland). For fluorescence-based screening, *E. coli* TOP 10 placEGFP was cultured in LB media (Roth, Germany) with 100 μg/mL ampicillin and 1 mM isopropyl β-D-thiogalactopyranoside IPTG (from Sigma-Aldrich, USA and Thermo Fischer Scientific, USA, respectively).

RESULTS AND DISCUSSION

Frequency of Screening. In screening microfluidics devices, droplets are analyzed one by one. In this case, splitting up a droplet is undesirable as it limits the resulting throughput of an assay, disrupting the correct readout. It has been shown that a small entrance angle to the detection channel and its width comparable to the droplet diameter is beneficial to increase the stable flow rate.[23] Compared to ref 22, we have reduced the entrance angle from 45 to 25°. Moreover, we have adjusted the channel width to fit the 1 nL droplet with a diameter of 120 μm (see Figure S1 for detailed microfluidic chip dimensions). Additionally, the frequency of
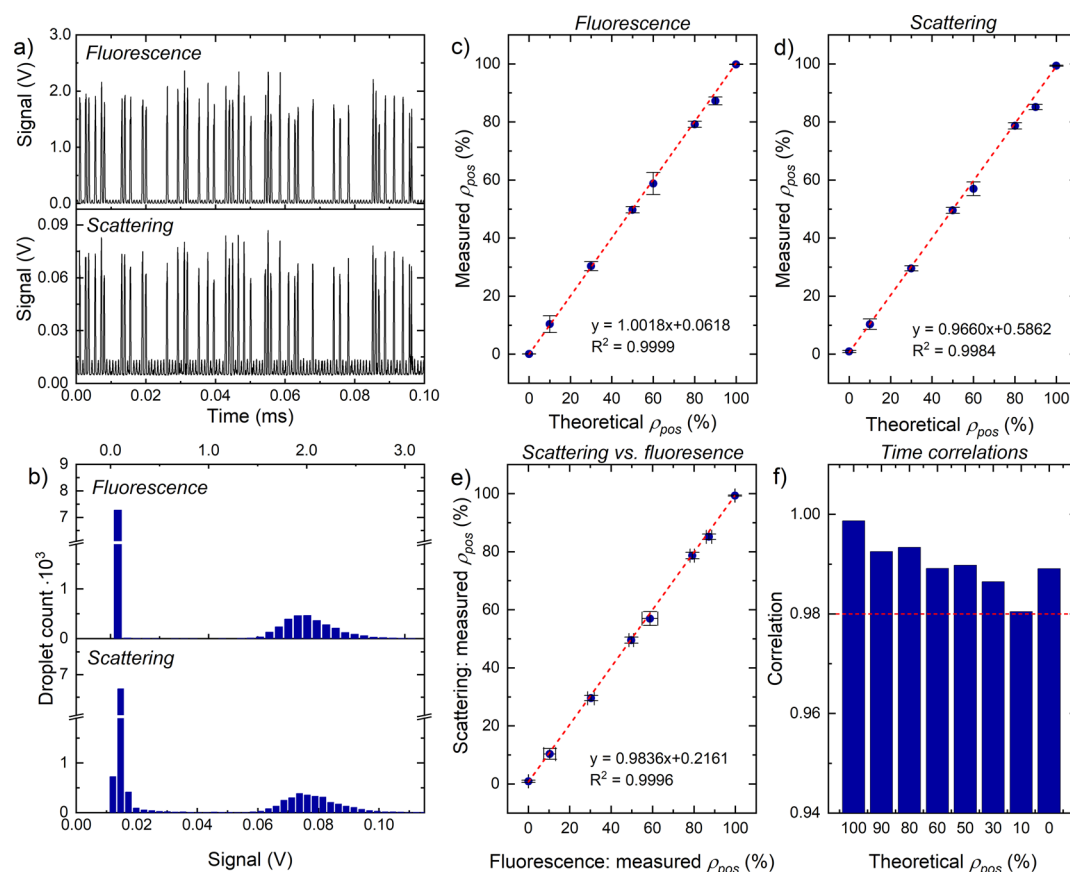
Figure 2. Validation of the label-free method, (a) fluorescence and scattered light signals from nanodroplets, (b) histograms of fluorescence and scattered light intensities, (c) correlation of theoretical and measured percentages of positive droplets determined by the method based on fluorescence intensity detection, (d) correlation of theoretical and measured percentages of positive droplets determined by detection of scattered light intensity, (e) comparison of fluorescence and scattered light detection in nanoliter droplets. Axes X and Y show the percentage quantity of positive droplets in the sample obtained by methods based on fluorescence and scattered light, respectively, (f) time correlation of signals of fluorescence and scattered light intensities.

screening depends not only on the total flow rate in the detection channel but also on the droplets' separation. Compared to the previous works based on the scattered light detection principle,[21,22] we have substantially reduced spacing oil between the droplets. The distance between each peak is kept minimal, as required for reliable droplet separation. This was obtained by optimizing the ratio of flow rates in oil and sample channels. This way, while maintaining the speed of droplet flow, we increased the number of droplets passed by the optical fiber in a given time, increasing the screening frequency. As a result, the setup allows for high-throughput droplet screening with a frequency of 1.2 kHz.

Validation of the Method. The monitoring of bacterial growth using fluorescent labeling is already a well-known and established technique. We compared our label-free assay with a fluorescent approach to validate our method, and for this purpose, we used genetically modified *E. coli* expressing a green fluorescent protein. We tested eight samples containing different percentages of empty droplets (ρ_{neg}) and the droplets containing a high concentration of bacteria, around 800 cells (ρ_{pos}). Those samples contained ρ_{pos} of 0, 10, 30, 50, 60, 80, 90, and 100% respectively. Each sample was analyzed in three replicates with the frequency of screening of 1.2 kHz. Figure 2a shows typical signals recorded in scattering and fluorescence channels; both are composed of peaks with high intensity (positive droplet) and low intensity (negative droplet). We

note that both signals are well correlated in time, that is, positive and negative droplets appear in both channels simultaneously. We counted the number of positive droplets using both scattering and fluorescence signals.

To distinguish positive and negative droplets, we used a simple two-level threshold-based approach. The first threshold (smaller one) allows us to count all the droplets in the sample and the second one (higher) to distinguish negative from positive compartments. In exemplary histogram plots, we can easily distinguish populations of negative (low peak intensity of signal) and positive (high peak intensity of signal) droplets (Figure 2b). Figure 2c,d shows the relationship between measured and theoretical percentages of positives droplets within each sample determined by detection of fluorescence and scattered light, respectively. As anticipated, the count of droplets judged as positive based on the fluorescent signal correlates tightly with the scattered light count. We found that the results of our label-free approach correlate highly with the fluorescence-based approach, as proved by the linear regression equation and coefficient of determination ($R^2 = 0.9996$) (Figure 2e). As we simultaneously record the scattered light and fluorescence signals, we further checked the time correlations between both signals. A correlation metric was proposed to represent the compatibility of a time distribution for different types of droplets. Each numerical value corresponding to a droplet's amplitude peak was converted

to 0 (for negative droplets) or 1 (for positive) depending on the maximum peak value. The previously defined threshold for differentiating positive and negative droplets was selected for assigning 0−1 labels for each trace. Now, we can check for compatibility of results in scattering and fluorescence traces for each consecutive droplet. Having such a label encoded representation, the correlation metric was calculated as the number of compliant pairs divided by the total number of droplets in the sample. We found out that the correlation coefficient is larger than 0.98 for each sample, as shown in Figure 2f. This shows that the detection of scattered light contains the same information as the detection of fluorescence.

Qualitative Readout of Bacterial Proliferation and Resolution of the Method. Phenotypic screening of bacteria in the droplets can be used for counting, antimicrobial susceptibility testing, population screening toward heterogeneity, or isolation of antibiotic-resistant bacteria. The crucial information from that experiment is the number of negative droplets and the number of droplets containing a dense population of bacteria. We tested our system for the ability to the qualitative screening of nonfluorescent, unmodified bacterial cells, that is, a possibility of distinguishing between empty and "full" droplets. We prepared samples containing different ratios of 1 nL droplets with growth medium only and the droplets with a very high concentration of *E. coli* (overnight culture, ~10^9 cfu/mL, which corresponds to around 1000 cells per droplet). We analyzed all samples at 1200 Hz (droplets/s) and determined the percentage quantity of two populations of the droplets. Figure 3a shows a high correlation between
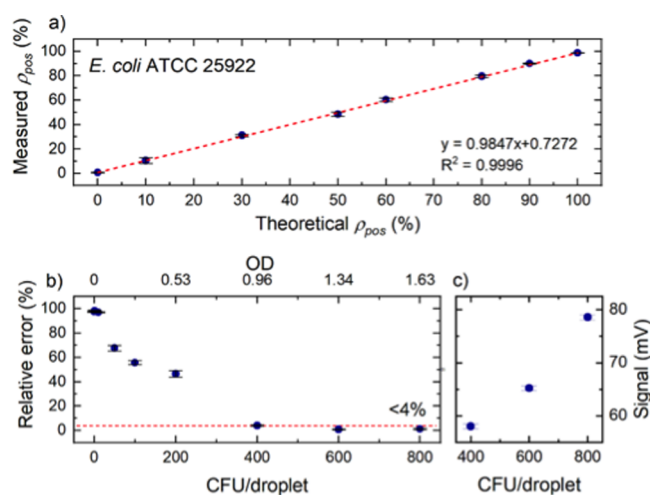

Figure 3. (a) Qualitative readout of nanoliter droplets based on scattered light. Axes *X* and *Y* indicate theoretical and measured percentage content of positive droplets in the sample, respectively. (b) Resolution of our assay. The graph presents relative error as a function of the number of bacteria cells per droplet. (c) Scattered signal intensity as a function of cell density.

prepared and measured contents of positives in the samples. We found out that the population of negative droplets without any cells is easily distinguishable from positive droplets containing a high concentration of bacteria and confirmed that we could perform a reliable readout in a label-free manner.

We also characterized the minimum number of bacteria in the droplet that could be reliably distinguished from an empty compartment. We prepared nine samples containing 30% of negatives and 70% of positives with a range of different

bacteria densities, from 1 to 800 cfu/droplet. For that purpose, we encapsulated different dilutions of *E. coli*. Figure 3b shows that a relative error of discrimination of positives from negatives is satisfactorily low for 400 cells per droplet or more. The relative error is an absolute error divided by the true number of positive droplets. Obtained results show that the droplet does not have to be completely full of bacterial cells to be treated as positive. An increase in cell concentration corresponds to the increased scattered signal intensity, as shown in Figure 3c.

Screening of Different Species of Bacteria. In principle, scattering-based detection should work with any species of bacteria. To verify this assumption, we tested six samples containing different fractions of negative and positive compartments with a high concentration of five different strains/species of bacteria: *S. aureus* LS1 and SH1000, *E. coli*, *P. aeruginosa*, *C. simulans*.

We chose bacteria that vary in size, shape (round-shape, rod-shape, and club-shape), and behavior (*S. aureus* SH1000 tends to form clamps). Those properties of scatters (i.e., bacterial cells) may affect the angle distribution of scattered light intensity. Figure 4 shows the results of the detection of positive droplets containing different strains or species of bacteria. In each case, we can observe a linear correlation between theoretical and measured percentages of positives within each sample, regardless of bacterial properties. Bacterial clamping causes slightly higher standard deviations, as seen in the case of *S. aureus* SH1000. We hypothesize that the aggregation of bacteria in the droplets can increase the number of false-positive signals. Besides, a potential limitation of using our system in microbiological experiments is the difficulty of encapsulation into droplets bacterial cells, which exhibit a filamentous phenotype or grow slowly. These features significantly constrict bacterial analysis at a single-cell level, and in the case of slow growers, the detection becomes impossible after a particular time of incubation because of limited droplet stability.

Furthermore, we also tested *S. intermedius*, *K. pneumoniae*, *A. baumanii*, *S. arizonae*, *S. sonnei*, and *L. monocytogenes*. We analyzed one sample for each strain. It contained 70% of negative droplets and 30% of positive compartments with a high number of tested cells (overnight culture). Figure S2 presents exemplary droplet signals for all bacteria, showing high contrast in peak intensities between positive and negative droplets.

Bacterial Proliferation in Droplets. We checked the possibility of using droplets as bioreactors for the proliferation of bacteria. We also determined the incubation time of the droplets required for *E. coli* to grow enough to distinguish positive droplets from negative ones. We encapsulated bacteria in that way to have a single cell per droplet, and then, we incubated the samples at 37 °C (see Figure 1b for single-cell experimental workflow). We diluted bacteria to the concentration, which, based on Poisson distribution, results in around 20% of positive compartments. We monitored the bacterial proliferation in time by determining the percentage of positive droplets based on scattered light intensity. We found out that the measured percentage of positives saturates at the level of 23.7% after 5 h. For this particular strain, this is the minimum time of incubation required to detect all positives in the sample (Figure 5a). Histogram plots (Figure 5b−d) show the changes observed in the number of negative and positive droplets and their peak intensities over time. Before incubation (0 h), only
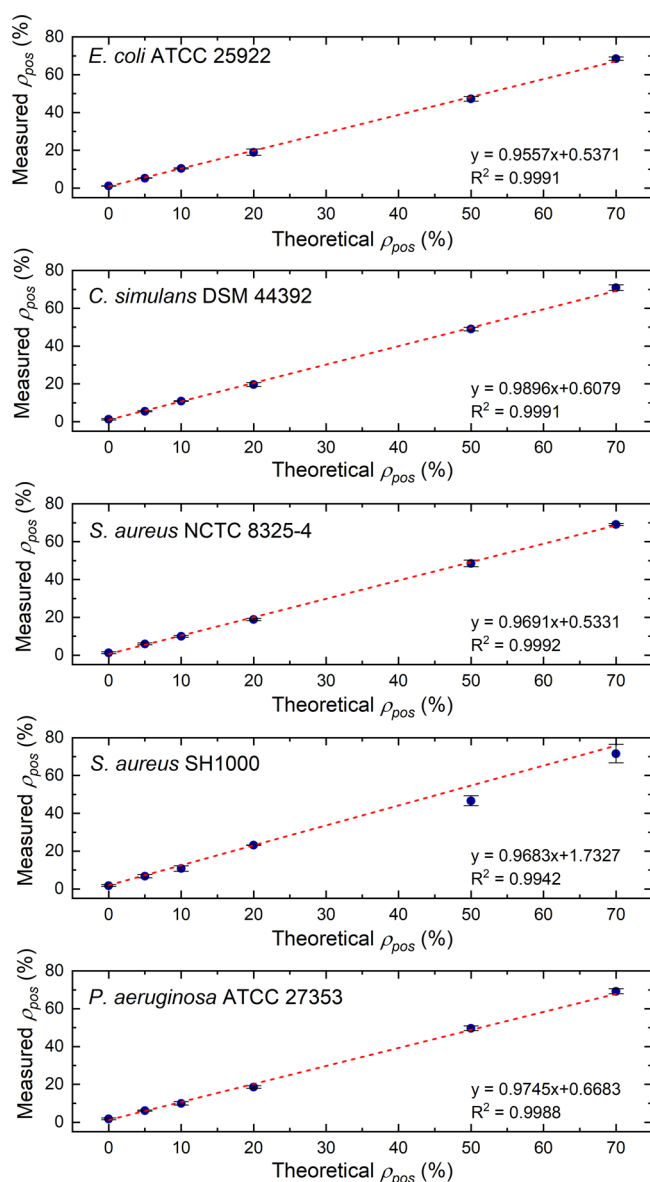
Figure 4. Ability to detect positive droplets containing different strains/species of bacteria. Axes *X* and *Y* indicate theoretical and measured percentage content of positive droplets in the sample, respectively.

Figure 5. Bacterial proliferation in the nanoliter droplets, (a) graph showing the percentage of positive droplets as a function of time and (b−d) histograms of scattered light intensity after 0, 8, and 24 h of incubation at 37 °C, respectively.

negative droplets were observed in the sample. After 8 and 24 h, a fraction of the droplets, which are full of cells, is visible, and the population of positives is easily distinguishable from negatives. As seen in Figure 5c,d, the average signal intensity of positive droplets grows in time, which is associated with an increasing number of cells inside the droplets during the incubation. The average scattered light intensities equal 75.6 ± 2.0, 117.1 ± 13.0, and 232.8 ± 18.4 mV after 5, 8, and 24 h of incubation, respectively. We observed that variability in signal values of positive droplets increases with time. It can be related to the phenotypic diversity of cells and various growth of bacteria in the droplets. A shift in the peak value toward higher intensities is visible between 8 and 24 h of incubation. This is associated with the continuous proliferation of cells within positive droplets (i.e., more scatters give higher scattered light intensity), but the percentage of positive droplets remains unchanged (as seen in Figure 5a).
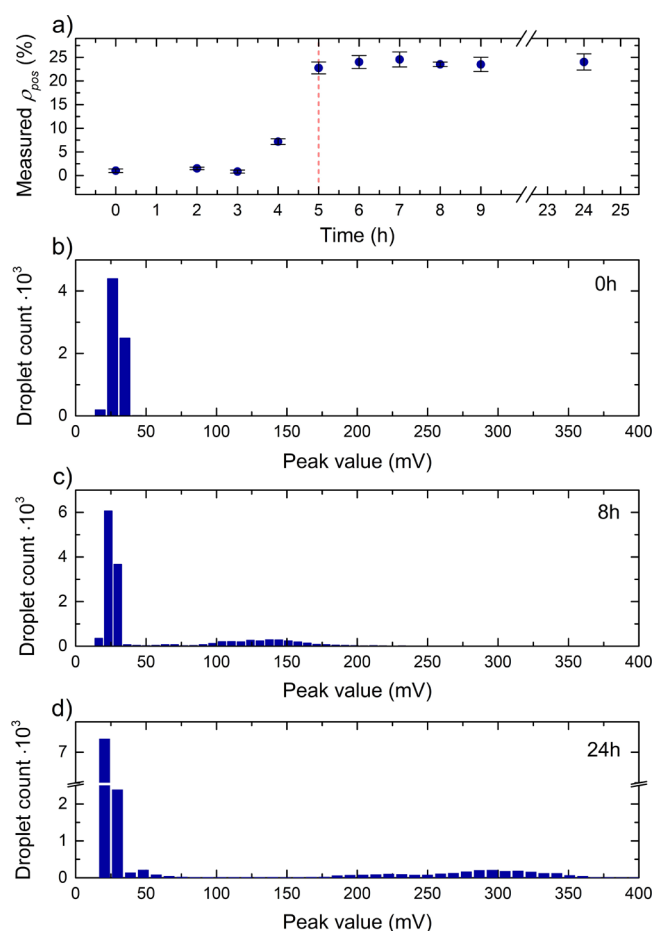
Screening of Bacteria toward Heterogeneity. Droplet microfluidics gives an opportunity for single-cell analysis and characterization of the response of individual cells to antibiotics. Our label-free system can thus be used to screen bacteria toward phenotypic heterogeneity. First, we determined the scMIC—that is, the average value of the minimum inhibitory concentration measured for individual cells encapsulated in droplets. We tested gentamicin against *S. aureus* LS1, which is a versatile pathogen causing a range of serious infections. Gentamicin was chosen because it is an antibiotic causing heterogeneous growth of *S. aureus*.[24,25] Figure 6 shows the decrease of bacterial viability with increased antibiotic concentration with complete inhibition of growth at 1 μg/mL of gentamicin.

Next, we treated bacteria with a narrow range of antibiotic concentrations, emphasizing the subMIC area, where cells' heterogeneous behavior is most likely to be observed. Figure 7a presents a fraction of resistant bacteria in the population F_R (*c*) depending on the antibiotic concentration *c*. We fit the data with the Gompertz function. We can observe that in one population, cells are responding differently to the same antibiotic. It is presented in Figure 7b, which shows the distribution of the probability of individual MIC in the population of bacteria (see Supporting Information for more details concerning methods of data analysis). The curve was obtained from a derivative of the data presented in Figure 7a.
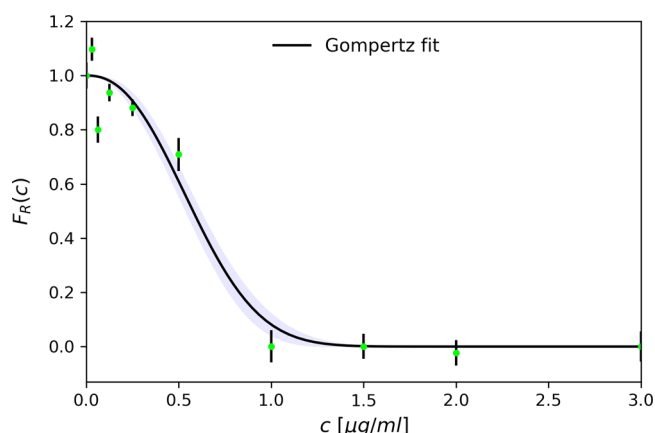
Figure 6. scMIC determination. The graph shows the change of bacterial viability in the form of the percentage content of positive droplets in a sample as a function of antibiotic concentration, normalized by the percent content of positives incubated without antibiotics. The shaded area shows errors related to the curve fitting parameters determined by the least-squares method.
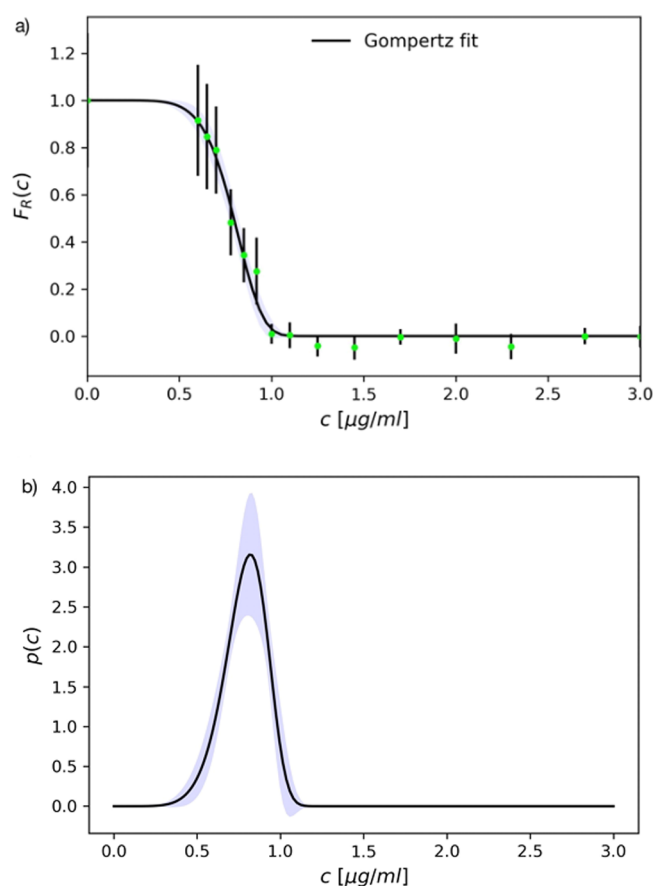

Figure 7. Analysis of bacteria population, (a) fraction of resistant bacteria in the population as a function of an antibiotic concentration and (b) probability density distribution of individual MIC in the population of bacteria.

We observed not a single value but a range of antibiotic concentrations, which inhibit bacteria's growth. Our future studies include the comparison of bacterial growth response after treatment with different antibiotics.

We can observe some negative values of the fraction of resistant bacteria in Figures 6 and 7a. They are not a result of

measurement in the experiment, but it is related to data analysis upon droplet detection. We always see some percentage of false positives, around 1.5%, and to provide more reliable results, we apply a mathematical model (see Supporting Information for details) to remove false-positive droplets from our data.

It is crucial to test the heterogeneity of the bacterial population because it can strongly affect the antibiotic treatment of a patient. There is a risk that it will be effective only for some part of the bacterial population. We believe that our system can also detect persistent cells, such as small colony variants, but further studies have to be performed.

■ CONCLUSIONS

Currently, a high throughput detection of the proliferation of bacterial cells in nanoliter droplets requires either addition of chemical dyes—markers of metabolic or enzymatic activity—that may leak out of the droplets or the use of genetically modified bacteria that express fluorescent proteins—that excludes the droplet techniques from being applied to species of practical interest in clinical or industrial settings. Our system provides a label-free readout of bacterial proliferation in the droplets with a high frequency of 1.2 kHz. We verified that scattering detection offered the same information as fluorescence analysis and tested the system's applicability for the label-free screening of 12 different bacterial species. We demonstrated the application of the method for determining the scMIC and detection of bacteria toward heterogeneity. The proposed system can be used for bacterial counting, antimicrobial susceptibility testing, selection of antibiotic-resistant bacteria, and screening toward heterogeneity of bacterial population.

■ ASSOCIATED CONTENT

ⓢ Supporting Information

The Supporting Information is available free of charge at https://pubs.acs.org/doi/10.1021/acs.analchem.0c03408.

> Schemes of microfluidic chips for droplet generation and reading, exemplary droplet signals recorded in scattering channel, and numerical analysis of data toward heterogeneity (PDF)

■ AUTHOR INFORMATION

Corresponding Author

Piotr Garstecki − *Institute of Physical Chemistry, Polish Academy of Sciences, 01-224 Warsaw, Poland;* ⓞ orcid.org/0000-0001-9101-7163; Email: garst@ichf.edu.pl

Authors

Natalia Pacocha − *Institute of Physical Chemistry, Polish Academy of Sciences, 01-224 Warsaw, Poland*

Jakub Bogusławski − *International Centre for Translational Eye Research, Institute of Physical Chemistry, Polish Academy of Sciences, 01-224 Warsaw, Poland*

Michał Horka − *Institute of Physical Chemistry, Polish Academy of Sciences, 01-224 Warsaw, Poland*

Karol Makuch − *Institute of Physical Chemistry, Polish Academy of Sciences, 01-224 Warsaw, Poland; Division of Chemistry and Chemical Engineering, California Institute of Technology, Pasadena, California 91125, United States*

Kamil Liżewski − *International Centre for Translational Eye Research, Institute of Physical Chemistry, Polish Academy of Sciences, 01-224 Warsaw, Poland*

Maciej Wojtkowski − *International Centre for Translational Eye Research, Institute of Physical Chemistry, Polish Academy of Sciences, 01-224 Warsaw, Poland*

Complete contact information is available at:
https://pubs.acs.org/10.1021/acs.analchem.0c03408

Author Contributions

N.P. and J.B. contributed equally. The manuscript was written through contributions of all authors. All authors have given approval to the final version of the manuscript.

Notes

The authors declare no competing financial interest.

REFERENCES

(1) Hindson, B. J.; Ness, K. D.; Masquelier, D. A.; et al. *Anal. Chem.* **2011**, *83*, 8604−8610.

(2) Macosko, E. Z.; Basu, A.; Satija, R.; et al. *Cells* **2015**, *161*, 1202−1214.

(3) Boedicker, J. Q.; Vincent, M. E.; Ismagilov, R. F. *Angew. Chem., Int. Ed.* **2009**, *48*, 5908−5911.

(4) Scheler, O.; Pacocha, N.; Debski, P. R.; Ruszczak, A.; Kaminski, T. S.; Garstecki, P. *Lab Chip* **2017**, *17*, 1980−1987.

(5) Lyu, F.; Pan, M.; Patil, S.; Wang, J.-H.; Matin, A. C.; Andrews, J. R.; Tang, S. K. Y. *Sens. Actuators, B* **2018**, *270*, 396−404.

(6) Scheler, O.; Makuch, K.; Garstecki, P.; Debski, P. R.; et al. *Sci. Rep.* **2020**, *10*, 3282.

(7) PostekW.Microfluidic screening of antibiotic susceptibility at a single-cell level shows inoculum effect of cefotaxime in E.coliLab on a Chip20182702396404

(8) Scheler, O.; Debski, P. R.; Horka, M.; Ruszczak, A.; Pacocha, N.; Postek, W.; Makuch, K.; Garstecki, P. Antibiotic inhibition of bacteria growth in droplets reveals heteroresistance pattern at the single cell level. **2016**, BioRxiv 328393.

(9) Kaminski, T. S.; Scheler, O.; Garstecki, P. *Lab Chip* **2016**, *16*, 2168−2187.

(10) Amstad, E.; Chemama, M.; Eggersdorfer, M.; Arriaga, L. R.; Brenner, M. P.; Weitz, D. A. *Lab Chip* **2016**, *16*, 4163−4172.

(11) Conchouso, D.; Castro, D.; Khan, S. A.; Foulds, I. G. *Lab Chip* **2014**, *14*, 3011−3020.

(12) Nisisako, T.; Torii, T. *Lab Chip* **2008**, *8*, 287−293.

(13) Yadavali, S.; Jeong, H.-H.; Lee, D.; Issadore, D. *Nat. Commun.* **2018**, *9*, 1222.

(14) Courtois, F.; Olguin, L. F.; Whyte, G.; Theberge, A. B.; Huck, W. T. S.; Hollfelder, F.; Abell, C. *Anal. Chem.* **2009**, *81*, 3008−3016.

(15) Chen, Y.; Gani, A.; Wijaya Gani, S. K. Y. *Lab Chip* **2012**, *12*, 5093−5103.

(16) Stapleton, J. A.; Swartz, J. R. *PLoS One* **2010**, *5*, No. e15275.

(17) Boitard, L.; Cottinet, D.; Kleinschmitt, C.; Bremond, N.; Baudry, J.; Yvert, G.; Bibette, J. *Proc. Natl. Acad. Sci. U.S.A.* **2012**, *109*, 7181−7186.

(18) Liao, D. S.; Raveendran, J.; Golchi, S.; Docoslis, A. *Sens. Bio. Sens. Res.* **2015**, *6*, 59−66.

(19) Jakiela, S.; Kaminski, T. S.; Cybulski, O.; Weibel, D. B.; Garstecki, P. *Angew. Chem., Int. Ed.* **2013**, *52*, 8908−8911.

(20) Zang, E.; Brandes, S.; Tovar, M.; Martin, K.; Mech, F.; Horbert, P.; Henkel, T.; Figge, M. T.; Roth, M. *Lab Chip* **2013**, *13*, 3707−3713.

(21) Liu, X.; Painter, R. E.; Enesa, K.; Holmes, D.; Whyte, G.; Garlisi, C. G.; Monsma, F. J., Jr.; Rehak, M.; Craig, F. F.; Smith, C. A. *Lab Chip* **2016**, *16*, 1636−1643.

(22) Hengoju, S.; Wohlfeil, S.; Munser, A. S.; Boehme, S.; Beckert, E.; Shvydkiv, O.; Tovar, M.; Roth, M.; Rosenbaum, M. A. *Biomicrofluidics* **2020**, *14*, 024109.

(23) Rosenfeld, L.; Fan, L.; Chen, Y.; Swoboda, R.; Tang, S. K. Y. *Soft Matter* **2014**, *10*, 421.

(24) Edwards, A. M. *J. Bacteriol.* **2012**, *194*, 5404−5412.

(25) Vulin, C.; Leimer, N.; Huemer, M.; Ackermann, M.; Zinkernagel, A. S. *Nat. Commun.* **2018**, *9*, 4074.